



ThMn₁₂-type structure and uniaxial magnetic anisotropy in ZrFe₁₀Si₂ and Zr_{1-x}Ce_xFe₁₀Si₂ alloys



A.M. Gabay^{*}, G.C. Hadjipanayis

Department of Physics and Astronomy, University of Delaware, Newark, DE, 19716, USA

ARTICLE INFO

Article history:

Received 14 September 2015

Received in revised form

5 October 2015

Accepted 7 October 2015

Available online xxx

Keywords:

Intermetallics

Permanent magnets

Crystal structure

Anisotropy

ABSTRACT

Arc-melted (Zr_{1-x}Ce_x)₁₁Fe₁₀Si₂ alloys were found to crystallize into a pure or nearly pure ThMn₁₂ structure for $0 \leq x \leq 0.6$. At room temperature, the alloys exhibit ferromagnetism with an uniaxial magnetocrystalline anisotropy. Metastable ZrFe₁₀Si₂ compound possesses room-temperature saturation magnetization of at least 11 kG and Curie temperature of 325 °C; both properties slightly decrease when Ce is being substituted for Zr. The anisotropy field, on the other hand, increases with the Ce from 16.9 to 24 kOe at $x = 0.6$. These intrinsic magnetic characteristics as well as the absence of expensive rare-earths and Co make the compounds interesting for development of low-cost permanent magnets. At $0.7 \leq x \leq 0.8$, the ThMn₁₂ structure was found to co-exist with the Th₂Ni₁₇-type structure, whereas the equilibrium Th₂Zn₁₇-type structure was observed only at $x = 1$. Prepared under similar conditions Hf₁₁Fe₁₀Si₂ alloy does not crystallize into the ThMn₁₂-type structure.

© 2015 Elsevier B.V. All rights reserved.

1. Introduction

Tetragonal R(Fe,M)₁₂ compounds with R standing for rare earth elements have long been of interest as permanent magnet materials [1]. In recent years, concerns about supply of the raw rare earths motivated intensifying search for the rare-earth-lean and rare-earth-free hard magnetic materials which would not necessarily surpass the Nd₂Fe₁₄B, but nevertheless could “bridge” the performance gap presently existing between the ferrite and Nd–Fe–B magnets [2]. The R(Fe,M)₁₂ compounds are already “rare-earth-lean” compared to the R–Fe–B and R–Co permanent magnet materials. To fully explore this advantage, a particular attention has been recently paid to synthesis of these compounds with the most abundant and least “critical” rare earth, cerium [3–5]. Although the mixed-valent state of the Ce atoms is known to have an unfavorable effect on the Curie temperature T_C of the Ce–Fe compounds, Zhou et al. [4] reported an unexpectedly high T_C of the 1:12 structure (the ThMn₁₂ type) in CeFe₁₀Si₂ – together with a uniaxial, if not very strong, magnetocrystalline anisotropy. This important observation was made for the multiphase alloy prepared via melt spinning, a non-equilibrium technique. *Ab initio* calculations by Drebov et al.

[6] had led to a tentative conclusion that the tetragonal CeFe₁₀Si₂ structure is stable. At the same time, the available experimental data [7–12] confirm stability of the tetragonal R(Fe,Si)₁₂ structures only for the rare-earth and actinide R having an atomic radius equal or smaller than 0.181 nm (Sc, Y, Sm, Gd, Tb, Dy, Ho, Er, Tm, Lu and U). Sakurada et al. [13] proposed a model according to which stability of the 1:12 structure in the R(Fe,Si)₁₂ alloys depends on the average radius of the atoms in the R sites (the 2a sites); they demonstrated stabilization of this structure when part of the larger Nd atoms in the RFe₁₀Si₂ was replaced with the smaller Zr atoms. The 1:12-structure-stabilizing effect of Zr is evident even in the case of the Sm atoms (the “borderline” atomic radius of 0.181 nm): unlike the SmFe₁₀Si₂, cast Sm_{0.7}Zr_{0.3}Fe₁₀Si₂ alloys were found to crystallize directly into the 1:12 structure [14]. In fact, Zr and Hf are the only non-rare-earth and non-actinide R known to form the tetragonal R(Fe,M)₁₂ compounds. However, the two such compounds reported to date, ZrFe_{12-δ}Al_δ and HfFe_{12-δ}Al_δ, exist at large δ values (6–7) and they do not exhibit a room-temperature ferromagnetism [15]. As for the Zr–Fe–Si system, the available phase diagrams [16,17] feature no equilibrium 1:12 structure at 800 °C, 1000 °C and 1100 °C.

The work presented in this report began as an attempt to study Zr substitution for Ce in the CeFe₁₀Si₂ alloys. To the authors' surprise, the 1:12 structure was easily obtained not only in the quaternary alloys, but also in the ternary ZrFe₁₀Si₂. Thus, the magnetic properties of the new Zr_{1-x}Ce_xFe₁₀Si₂ series of the 1:12 compounds

^{*} Corresponding author. University of Delaware, 217 Sharp Lab, Newark, DE, 19716, USA.

E-mail address: gabay@udel.edu (A.M. Gabay).

are reported together with discussion of their stability and application prospects.

2. Experiment

Alloys with the nominal compositions $(\text{Zr}_{1-x}\text{Ce}_x)_{8.4}\text{Fe}_{76.2}\text{Si}_{15.4}$ with $x = 0, 0.2, 0.4, 0.6, 0.7, 0.8, 1.0$ and also a $\text{Hf}_{8.4}\text{Fe}_{76.2}\text{Si}_{15.4}$ alloy were prepared as 2.5 g ingots by arc-melting the pure components on a water-cooled copper hearth. Selected alloys were additionally annealed at 1000 °C (in argon-filled quartz capsules; quenched in water). Ingot surfaces, likely to contain impurities, were machined off prior to characterization. Densities of the alloys were determined with the water-immersion techniques (the Archimedes method). Powders for X-ray diffraction (XRD) and room-temperature magnetic measurements were prepared with a hand mortar. Oriented powders were immobilized with epoxy resin (for the XRD) or with paraffin wax (for the magnetic measurements) under a magnetic field of 16–19 kOe. XRD determination of the crystal phases was performed with a Rigaku Ultima IV diffractometer at the CuK α radiation. The XRD results were analyzed with Powder Cell software [18]. Scanning electron microscopy (SEM; a JEOL JSM-6335F instrument) and energy-dispersive spectrometry (EDS; an IXRF Systems instrument) of polished unetched alloy samples were employed to clarify the nature of minority phases. The magnetic measurements were done with a Quantum Design VersaLab vibrating sample magnetometer. Thermomagnetic data were obtained at a field of 5 kOe for small (≈ 10 mg) ingot pieces. Room-temperature magnetization-vs-field data for the oriented powders were corrected for self-demagnetization using

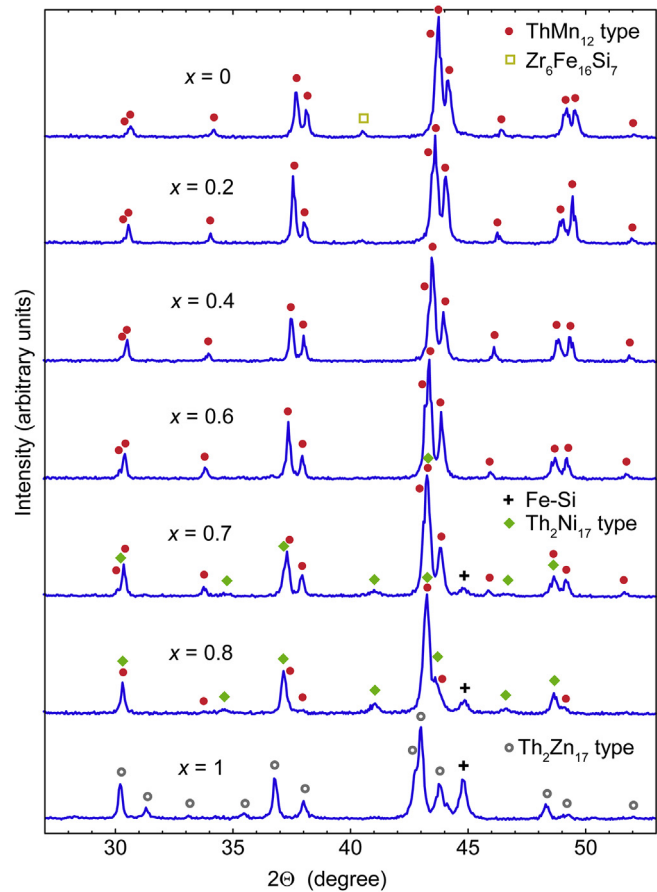


Fig. 1. Powder XRD spectra of $(\text{Zr}_{1-x}\text{Ce}_x)_{1.1}\text{Fe}_{10}\text{Si}_2$ arc-melted alloys.

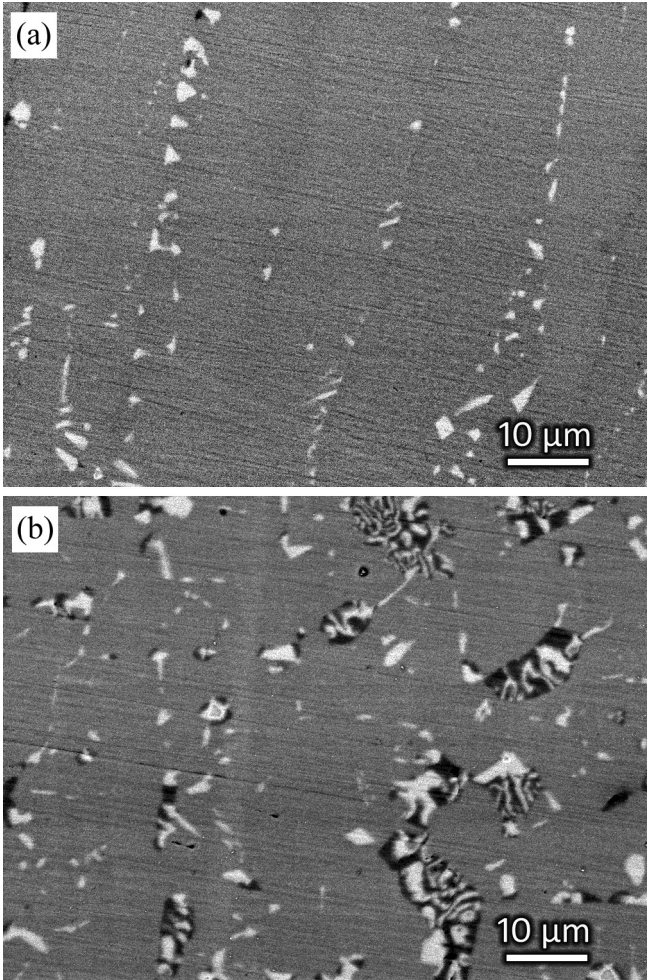


Fig. 2. Backscattered electrons SEM micrographs of $\text{Zr}_{1.1}\text{Fe}_{10}\text{Si}_2$ arc-melted alloy: (a) as-made, (b) additionally annealed for 20 h at 1000 °C. Lighter inclusions: $\text{Zr}_{19}\text{Fe}_{57}\text{Si}_{24}$; darker inclusions: $\text{Fe}_{88}\text{Si}_{12}$.

demagnetization factors determined for similarly prepared Fe powders.

3. Results

XRD spectra of the as-made alloys are presented in Fig. 1. The ternary $\text{ZrFe}_{10}\text{Si}_2$ sample features the 1:12 structure coexisting with 3–5 vol.% of the cubic $\text{Zr}_6\text{Fe}_{16}\text{Si}_7$ structure (the $\text{Mg}_6\text{Cu}_{16}\text{Si}_7$ type, space group $\text{Fm}\bar{3}\text{m}$, $a = 1.157$ nm). The latter phase appears as lighter inclusions in the backscattered electrons SEM image shown in Fig. 2(a). The 1:12 becomes the only detectable structure in the Ce-substituted $(\text{Zr}_{1-x}\text{Ce}_x)_{1.1}\text{Fe}_{10}\text{Si}_2$ alloys when $0.2 \leq x \leq 0.6$. Further Ce substitution results in emergence of $(\text{Ce,Zr})_2(\text{Fe,Si})_{17}$ and

Table 1
Approximate volume percentage of crystalline phases observed in arc-melted $(\text{Zr}_{1-x}\text{Ce}_x)_{1.1}\text{Fe}_{10}\text{Si}_2$ alloys with $x \geq 0.6$.

x	Structure			
	1:12	2:17H	2:17R	bcc
0.6	100	0	0	0
0.7	57	36	0	7
0.8	24	69	0	7
1.0	0	0	79	21

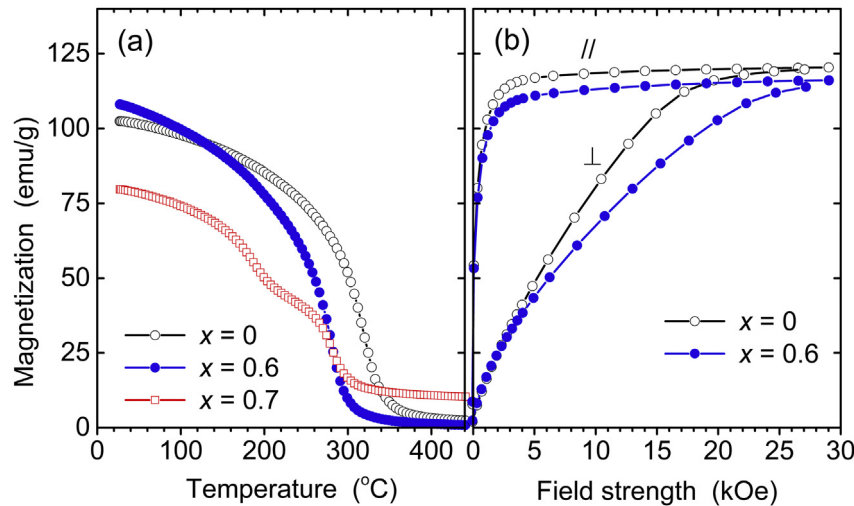


Fig. 3. Magnetization of selected $(\text{Zr}_{1-x}\text{Ce}_x)_{1.1}\text{Fe}_{10}\text{Si}_2$ arc-melted alloys: (a) heating alloy pieces at 5 kOe; (b) room-temperature isotherms for field-oriented powders in parallel (//) and perpendicular (\perp) directions.

bcc Fe–Si phases. It is interesting that in none of the alloys the 1:12 structure was found to be present alongside the rhombohedral $\text{Th}_2\text{Zn}_{17}$ -type structure (2:17R) which is the equilibrium structure of the $\text{Ce}_2(\text{Fe},\text{Si})_{17}$ compounds [19]. At $0.7 \leq x \leq 0.8$, the $(\text{Ce},\text{Zr})_2(\text{Fe},\text{Si})_{17}$ phase in the arc-melted $(\text{Zr}_{1-x}\text{Ce}_x)_{1.1}\text{Fe}_{10}\text{Si}_2$ alloys adopts the hexagonal $\text{Th}_2\text{Ni}_{17}$ -type structure (2:17H) with the lattice parameters $a \approx 0.84$ nm and $c \approx 0.83$ nm. Only the Zr-free $\text{Ce}_{1.1}\text{Fe}_{10}\text{Si}_2$ alloy featured the 2:17R as the majority phase – and it showed no traces of the 1:12 structure. The quantitative XRD estimates for the phases observed on the Ce side of the alloy series are summarized in Table 1; these results are corroborated by the SEM-EDS data.

Although there exist $\text{Hf}(\text{Fe},\text{Al})_{12}$ compounds isotypical to the $\text{Zr}(\text{Fe},\text{Al})_{12}$ [15], the arc-melted $\text{Hf}_{1.1}\text{Fe}_{10}\text{Si}_2$ alloy did not contain the 1:12 structure. Instead, the alloy was found to crystallize into a

mixture of the bcc Fe–Si phase (60–70 vol.%) and the Laves phase Hf–Fe–Si (the MgZn_2 -type, $\text{P6}_3/\text{mmc}$) with $a \approx 0.486$ nm and $c \approx 0.791$ nm.

Thermomagnetic scans, some of which are presented in Fig. 3(a), confirm that the 1:12 phase is the only ferromagnetic phase present in the $(\text{Zr}_{1-x}\text{Ce}_x)_{1.1}\text{Fe}_{10}\text{Si}_2$ alloys with $0 \leq x \leq 0.6$. Its Curie temperature T_C decreases with the Ce substitution from 325 °C to 285 °C. At $x = 0.7$, the magnetization of the 1:12 phase is significantly diluted by two other ferromagnetic phases, 2:17H exhibiting a T_C of around 200 °C and Fe–Si ($T_C > 450$ °C).

The easy magnetization direction (EMD) of the tetragonal 1:12 structure in the arc-melted $(\text{Zr}_{1-x}\text{Ce}_x)_{1.1}\text{Fe}_{10}\text{Si}_2$ alloys was determined by comparing the XRD spectra recorded for randomly oriented and field-oriented powder samples (data 1 and 2 in Fig. 4).

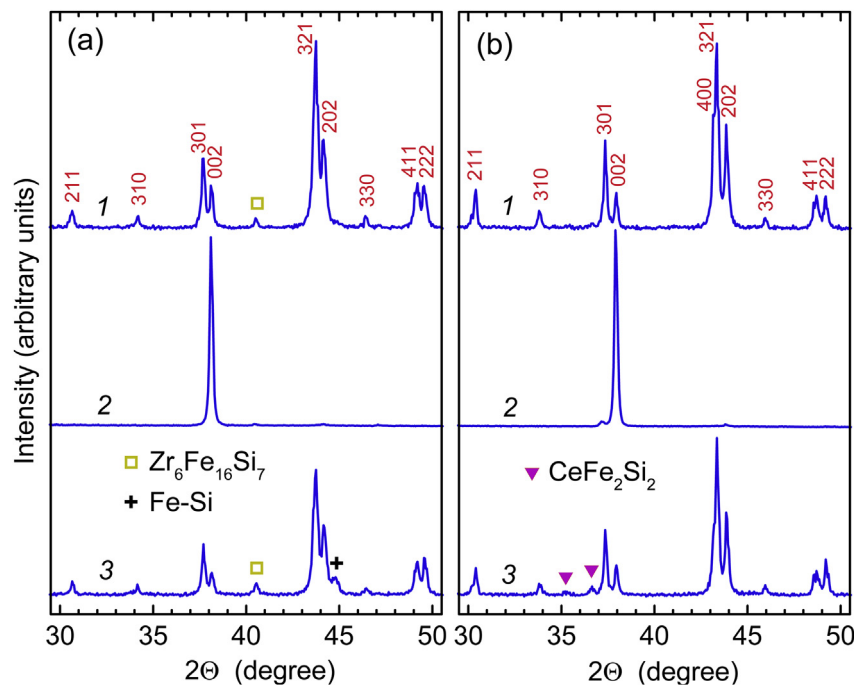


Fig. 4. Powder XRD spectra of (a) $\text{Zr}_{1.1}\text{Fe}_{10}\text{Si}_2$ and (b) $(\text{Zr}_{0.4}\text{Ce}_{0.6})_{1.1}\text{Fe}_{10}\text{Si}_2$ arc-melted alloys: 1 – randomly oriented; 2 – field-oriented; 3 – randomly oriented after additional annealing for 20 h at 1000 °C.

Table 2

Lattice parameters, density, Curie temperature, room-temperature saturation magnetization and anisotropy field of $(\text{Zr}_{1-x}\text{Ce}_x)_{1.1}\text{Fe}_{10}\text{Si}_2$ alloys crystallized into the ThMn_{12} -type structure.

x	a (nm)	c (nm)	ρ (g/cm ³)	T_C (°C)	$4\pi M_s$ (kG)	H_a (kOe)
0 ^a	0.8300	0.4721	7.26	325	11.0	16.9
0.2	0.8322	0.4724	7.30	304	11.1	18.7
0.4	0.8356	0.4740	7.34	289	10.8	21.3
0.6	0.8376	0.4741	7.36	285	10.8	24.0

^a Alloy contains up to 5 vol.% of non-magnetic $\text{Zr}_6\text{Fe}_{16}\text{Si}_7$ phase.

The very strong enhancement of the [002] reflections at the expense the $[hkl]$ with $h, k \neq 0$ conclusively demonstrates that the magnetocrystalline anisotropy of the $\text{Zr}_{1-x}\text{Ce}_x\text{Fe}_{10}\text{Si}_2$ compounds is uniaxial. Magnetization curves measured parallel and perpendicular to the [001] EMD [the examples are shown in Fig. 3(b)] were used to determine room-temperature values of the anisotropy field H_a ; the H_a monotonically increases with the x reaching 24 kOe at $x = 0.6$. The saturation magnetization values $4\pi M_s$ were found by extrapolating the $M(1/H^2)$ data. The value determined this way for the $\text{Zr}_{1.1}\text{Fe}_{10}\text{Si}_2$ alloy, 11.0 kG, can only be considered a low $4\pi M_s$ estimate for the 1:12 $\text{ZrFe}_{10}\text{Si}_2$ compound, because it does not account for several percent of the non-magnetic $\text{Zr}_6\text{Fe}_{16}\text{Si}_7$ phase present in this alloy. The crystallographic and magnetic data for $\text{Zr}_{1-x}\text{Ce}_x\text{Fe}_{10}\text{Si}_2$ compounds are summarized in Table 2.

Based on the data for the Zr-Fe-Si equilibria [16,17], one can state with sufficient confidence that the observed $\text{ZrFe}_{10}\text{Si}_2$ compound is metastable. There is no, however, such certainty regarding the Ce-substituted compounds. Moreover, even relative stability during a heat treatment may be of interest for materials with application prospects. Therefore, two of the $(\text{Zr}_{1-x}\text{Ce}_x)_{1.1}\text{Fe}_{10}\text{Si}_2$ alloys, $x = 0$ and $x = 0.6$, were annealed for up to 20 h at 1000 °C. In both cases, most of the 1:12 phase (around 90%) has been preserved

(see XRD spectra 3 in Fig. 4). At the same time, the Fe–Si phase has emerged in the annealed $\text{Zr}_{1.1}\text{Fe}_{10}\text{Si}_2$ alloy, and the amount of the $\text{Zr}_6\text{Fe}_{16}\text{Si}_7$ phase has increased; the corresponding SEM micrograph is shown in Fig. 2(b). In the annealed alloy $x = 0.6$, the XRD (Fig. 4) and SEM-EDS (not shown) detected, somewhat unexpectedly, a Zr-free CeFe_2Si_2 minority phase (the Al_4Ba type, $I4/mmm$, $a = 0.399$ nm, $c = 0.986$ nm). There were no indications of emergence of the bcc Fe–Si phase.

4. Discussion

The findings presented in this report are reasonably consistent with the information available in the literature. The lattice parameters of the newly observed $\text{Zr}_{1-x}\text{Ce}_x\text{Fe}_{10}\text{Si}_2$ compounds agree with the values reported for $\text{CeFe}_{10}\text{Si}_2$ [4] (see Fig. 5). The agreement for the T_C values is less good, but the difference may be explained, at least in part, by the different methods of the thermomagnetic analysis. The “stabilizing” effect of Zr on the $\text{RFe}_{10}\text{Si}_2$ compounds [13,14] has been confirmed; moreover, the “stabilized” $(\text{R,Zr})_{1.1}\text{Fe}_{10}\text{Si}_2$ compounds may now be seen as an extension of the $\text{ZrFe}_{10}\text{Si}_2$.

Having a rather modest anisotropy constant $K_1 = H_a M_s / 2$ of $7.4 \cdot 10^6$ erg/cm³, the $\text{ZrFe}_{10}\text{Si}_2$ compound itself may not have a significant potential for the permanent magnet applications. However, as a new uniaxially anisotropic ferromagnet not containing rare earths or other “critical” elements [20] such as Co, it deserves attention as a possible base for low-cost permanent magnet materials superior to the barium ferrites. The Ce substitution may serve an example here; the $\text{Zr}_{0.4}\text{Ce}_{0.6}\text{Fe}_{10}\text{Si}_2$ contains as little as 11.4 wt.% of the most abundant rare earth, but its K_1 value reaches $1.03 \cdot 10^7$ erg/cm³ and its magnetic hardness parameter $(K_1 / 4\pi M_s^2)^{1/2}$ is equal to 1.05. The compound, therefore, meets the requirement proposed in Ref. [21] for a permanent magnet material to have its anisotropy energy higher than its magnetostatic energy. At the same time, the known past attempts to obtain an application-worthy magnetic hysteresis in the $\text{UFe}_{10}\text{Si}_2$ [10] and $\text{Sm}_{0.7}\text{Zr}_{0.3}\text{Fe}_{10}\text{Si}_2$ [14] exhibiting even higher H_a values were not very successful.

Development of a permanent magnet consists essentially in creating the specific favorable microstructure, usually via mechanical and thermal processing. This may be particularly difficult if the base compound is metastable; and many of the compounds derived from the $\text{ZrFe}_{10}\text{Si}_2$ are expected to be so. It is therefore significant that the $\text{Zr}_{1-x}\text{Ce}_x\text{Fe}_{10}\text{Si}_2$ compounds were mostly preserved after a prolonged heat treatment: this may allow for more options when actually attempting the development of practical magnets.

5. Conclusion

The metastable $\text{ZrFe}_{10}\text{Si}_2$ compound synthesized via arc-melting possesses the intrinsic properties of a moderately hard magnetic material. Its derivatives such as $\text{Zr}_{1-x}\text{Ce}_x\text{Fe}_{10}\text{Si}_2$ may be of interest for the development of new low-cost permanent magnets superior to the ferrite and Alnico magnets.

Acknowledgments

This work was supported by U.S. Department of Energy (Grant No. DE-FG02-04ERU612) and University of Delaware Energy Institute.

References

- [1] K.H.J. Buschow, Permanent magnet materials based on tetragonal rare earth

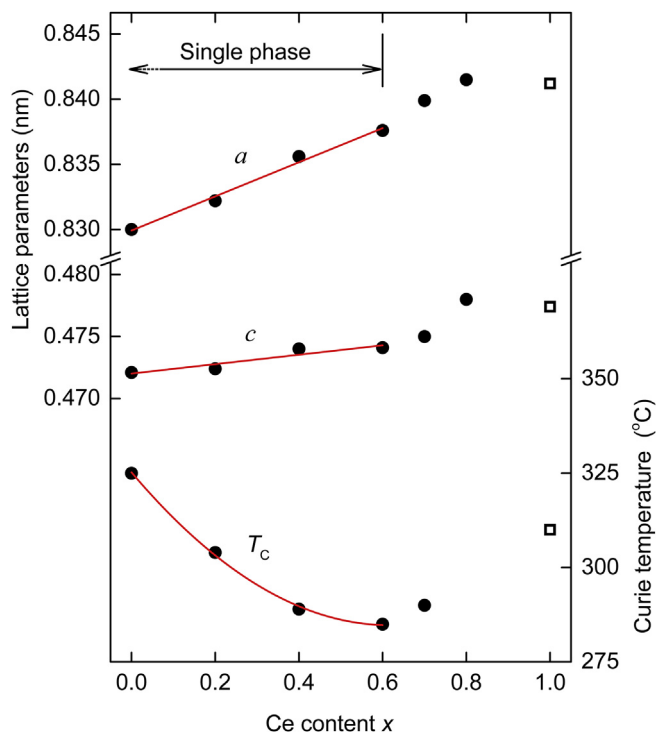


Fig. 5. Effect of Ce content on lattice parameters and Curie temperatures of the 1:12 phase in $(\text{Zr}_{1-x}\text{Ce}_x)_{1.1}\text{Fe}_{10}\text{Si}_2$ arc-melted alloys as found in this work (filled symbols) and reported in Ref. [4] (open symbols).

- compounds of the type $RFe_{12-x}M_x$, J. Magn. Magn. Mater. 100 (1991) 79–89.
- [2] J.M.D. Coey, Permanent magnets: plugging the gap, Scr. Mater. 67 (2012) 524–529.
 - [3] D. Goll, R. Loeffler, R. Stein, U. Pflanz, S. Goeb, R. Karimi, G. Schneider, Temperature dependent magnetic properties and application potential of intermetallic $Fe_{11-x}Co_xTiCe$, Phys. Status Solidi RRL 8 (2014) 862–865.
 - [4] C. Zhou, F.E. Pinkerton, J.F. Herbst, High Curie temperature of Ce-Fe-Si compounds with $ThMn_{12}$ structure, Scr. Mater. 95 (2015) 66–69.
 - [5] C. Zhou, K. Sun, F.E. Pinkerton, M.J. Kramer, Magnetic hardening of $Ce_{11+x}Fe_{11-y}Co_yTi$ with $ThMn_{12}$ structure by melt spinning, J. Appl. Phys. 117 (2015), 17A741 (1–4).
 - [6] N. Drebov, A. Martinez-Limia, L. Kunz, A. Gola, T. Shigematsu, T. Eckl, P. Gumbsch, C. Elsässer, Ab initio screening methodology applied to the search for new permanent magnetic materials, New J. Phys. 15 (2013), 125023 (1–24).
 - [7] K.H.J. Buschow, Structure and magnetic properties of some novel ternary Fe-rich rare-earth intermetallics, J. Appl. Phys. 63 (1988) 3130–3135.
 - [8] K. Ohashi, Y. Tawara, R. Osugi, M. Shimao, Magnetic properties of Fe-rich rare-earth intermetallic compounds with a $ThMn_{12}$ structure, J. Appl. Phys. 64 (1988) 5714–5716.
 - [9] P. Stefański, A. Werzeczono, Structural and magnetic properties of $RFe_{10}Si_2$ compounds, J. Magn. Magn. Mater. 82 (1989) 125–128.
 - [10] A.V. Andreev, S.V. Andreev, E.N. Tarasov, Magnetic properties $UFe_{12-x}Si_x$, J. Less-Common Metal. 167 (1991) 255–259.
 - [11] A.V. Andreev, M.I. Bartashevich, H. Aruga Katori, T. Goto, Magnetic anisotropy and magnetostriction of $UFe_{10}Si_2$, J. Alloys Compd. 216 (1994) 221–225.
 - [12] O.I. Bodak, J. Stepień-Damm, H. Drulis, B. Kotur, W. Suski, F.G. Vagizov, K. Wochowski, T. Mydlarz, Structure and magnetic properties of $ScFe_{10}Si_2$, Physica B 210 (1995) 183–189.
 - [13] S. Sakurada, A. Tsutai, M. Sahashi, A study on the formation of $ThMn_{12}$ and $NaZn_{13}$ structures in $RFe_{10}Si_2$, J. Alloys Compd. 187 (1992) 67–71.
 - [14] A.M. Gabay, N.N. Shchegoleva, E.V. Belozarov, The structure and hard magnetic properties of rapidly quenched $(Sm,Zr)_{11}(Fe,Si)_{12}$ alloys, Phys. Met. Metallogr. 94 (2002) 252–257.
 - [15] M.A. McGuire, N. Ghimire, D.J. Singh, Ferromagnetism in $ZrFe_{12-x}Al_x$ and $HfFe_{12-x}Al_x$ ($x = 6.0, 6.5, 7.0$), J. Appl. Phys. 111 (2012), 093918 (1–6).
 - [16] L.A. Lisenko, Z. Ban, E.I. Gladisevskii, Investigation of the system Zr-Fe-Si, Croat. Chem. Acta 43 (1971) 113–118.
 - [17] C.P. Wang, Y. Hu, S.Y. Yang, Y. Lu, Q.W. Jiang, X.J. Liu, Experimental investigation of phase equilibria in the Fe-Si-Zr ternary system, J. Phase Equilibria Diffus. 34 (2013) 277–288.
 - [18] W. Kraus, G. Nolze, Powder cell – a program for the representation and manipulation of crystal structures and calculation of the resulting X-ray powder patterns, J. Appl. Crystallogr. 29 (1996) 301–303.
 - [19] D.P. Middleton, K.H.J. Buschow, Magnetic properties of $Ce_2Fe_{17-x}Si_x$ compounds, J. Alloys Compd. 206 (1994) L1–L2.
 - [20] A.J. Hurd, R.L. Kelley, R.G. Eggert, M.H. Lee, Energy-critical elements for sustainable development, MRS Bull. 37 (2012) 405–410.
 - [21] R. Skomski, J.M.D. Coey, Permanent Magnetism, Taylor & Francis Group, New York, 1999, p. 159.